*Transactions of the Korean Nuclear Society Autumn Meeting*
*Gyeongju, Korea, October 29-30, 2015*

# Evaluation of Physical Characteristics of PWR Cores with Accident Tolerant Fuels

Dae Hee Hwang and Ser Gi Hong*, Wang Kee In[b]
*Department of Nuclear Engineering, Kyung Hee University*
*1732 Deogyeong-daero, Giheung-gu, Yongin-si, Gyeonggi-do, 446-701, Korea*
*[b]Korea Atomic Energy Research Institute, 989-111 Daedeok-daero, Yuseong-Gu, Daejeon 34057*
**Corresponding author: sergihong@khu.ac.kr*

## 1. Introduction

After the recent events at Fukushima Dai-ichi, the accident tolerant fuels (ATF) have been actively studied to improve the safety of reactor core by providing substantially improved response to a DBA or BDB accident. There are various concepts of new fuel and cladding materials which are tentatively being considered as ATF. The ATF considered in this work includes metallic microcell $UO_2$[1] pellets and outer Cr-based alloy coating[2] on cladding, which is being developed in KAERI (Korea Atomic Energy Research Institute). Chromium metals have been used in many fields because of its hardness and corrosion-resistance. The use of the chromium metal in nuclear fuel rod can enhance the conductivity of pellets and corrosion-resistance of cladding[1, 2]. The objective of this work is to study the neutronic performances and characteristics of the commercial PWR core loaded the ATF-bearing assemblies.

## 2. Computational Methods

DeCART2D (Deterministic Core Analysis based on Ray Tracing for 2-Dimensional Core) code[3] is used to analyze the fuel assemblies and to produce the two-group homogenized assembly cross sections. This code recently has been developed in KAERI to generate few group homogenized neutron cross section data for nodal diffusion core analysis code. Then, the table sets which includes functionalized group constants are produced by using the PROLOG program and HGC file prepared with DeCART2D. The calculations for core analysis are performed by using MASTER (Multi-purpose Analyzer for Static and Transient Effects of Reactors) code[4] which was developed in KAERI. MASTER is a nuclear analysis and design code which can simulate the pressurized water reactor (PWR) core or the boiling water reactor (BWR) core in 1-, 2-, or 3-dimensional Cartesian or hexagonal geometry with the advanced nodal diffusion methods.

## 3. Fuel Assembly and Reactor Core Design

In this work, it is determined that the ATF assemblies start to be loaded into the core from 8th cycle of Hanbit-3 nuclear power plant and three-batch refueling scheme is adopted for core loading pattern[5]. We considered four different cases using conventional uranium fuel and ATF assemblies. The CASE 1 uses the conventional $UO_2$ fuels while the uranium enrichments of 4.7wt% and 4.2wt% for the enrichment zoned fuels are determined to satisfy the cycle length of 480 EFPDs. On the other hand, the CASE 2, 3, and 4 use Cr-containing metallic microcell $UO_2$ pellets and Cr-based alloy outer coating on cladding. The only difference between ATF CASEs is the uranium enrichment. Table I shows the design data for comparison of the four CASEs in detail. The ATF pellets in the CASE 2, 3, and 4 include chromium of 3.34 wt% and the outer cladding thickness of 0.05 mm is replaced by Cr-based alloy. The uranium enrichment of the CASE 2 is same as the CASE 1 (i.e., the conventional $UO_2$ pellets) and the CASE 3 uses 4.95wt% uranium enrichment that is consider as the upper limit of uranium enrichment in PWRs. The enrichment of CASE 4 was selected to consider the core using ATF fuels which has the similar cycle length to the CASE 1 (i.e., 480 EFPDs) at the equilibrium cycle. As will be described in the following paragraph, we performed cycle-by-cycle reload core calculations including loading pattern search from the cycle 7 to the equilibrium cycle. The results showed that the cores considered in this work reached their equilibrium cycles at the 12th cycle. As shown in Table I, the uranium enrichments for zoned fuels were increased up to 5.20wt% and 4.7wt% to achieve 480EFPDs cycle length with ATF fuels. These degradations in the neutronic characteristic are due to the larger neutron absorption cross section of Cr than Zircaloy-4 and the smaller fuel inventories of ATF pellets.

Table I. Design data of fuel assembly for four CASEs

| | CASE 1 | CASE 2 | CASE 3 | CASE 4 |
|---|---|---|---|---|
| U enrichment[wt%] | 4.70/4.2 | 4.70/4.2 | 4.95/4.45 | 5.20/4.7 |
| Fuel pellet | $UO_2$ | $UO_2$-Cr | $UO_2$-Cr | $UO_2$-Cr |
| Pellet density [g/cc] | 10.176 | 10.140 | 10.140 | 10.140 |
| Pellet radius [cm] | 0.4095 | 0.4095 | 0.4095 | 0.4095 |
| Cladding material | Zircaloy-4 | Zircaloy-4 | Zircaloy-4 | Zircaloy-4 |
| Cladding thickness (+gap) [cm] | 0.0655 | 0.0605 | 0.0605 | 0.0605 |
| Coating material | - | Cr-based alloy | Cr-based alloy | Cr-based alloy |
| Coating thickness [cm] | - | 0.005 | 0.005 | 0.005 |
| Rod radius [cm] | 0.4750 | 0.4750 | 0.4750 | 0.4750 |
| Pin pitch [cm] | 1.2882 | 1.2882 | 1.2882 | 1.2882 |
| Assembly pitch [cm] | 20.879 | 20.879 | 20.879 | 20.879 |

Table II. The number of fuel assemblies used in each cycle

| **FA type** | **The number of fuel assemblies** | | | | | |
|---|---|---|---|---|---|---|
| | **Cycle 7** | **Cycle 8** | **Cycle 9** | **Cycle 10** | **Cycle 11** | **Cycle 12** |
| H0 | 20 | | | | | |
| H1 | 8 | | | | | |
| H2 | 21 | | | | | |
| J0 | 20 | 20 | | | | |
| J1 | 20 | 8 | | | | |
| J2 | 24 | 21 | | | | |
| K0 | 20 | 20 | 20 | | | |
| K1 | 20 | 20 | 12 | | | |
| K2 | 24 | 24 | 17 | | | |
| L0 | | 20 | 20 | 20 | | |
| L1 | | 20 | 20 | 9 | | |
| L2 | | 24 | 24 | 20 | | |
| M0 | | | 20 | 20 | 20 | |
| M1 | | | 20 | 20 | 9 | |
| M2 | | | 24 | 24 | 20 | |
| N0 | | | | 20 | 20 | 20 |
| N1 | | | | 20 | 20 | 9 |
| N2 | | | | 24 | 24 | 20 |
| O0 | | | | | 20 | 20 |
| O1 | | | | | 20 | 20 |
| O2 | | | | | 24 | 24 |
| P0 | | | | | | 20 |
| P1 | | | | | | 20 |
| P2 | | | | | | 24 |
| **Total** | 177 | 177 | 177 | 177 | 177 | 177 |

Table III. Specification of the fuel assemblies for CASE 1

| **FA type** | **Uranium enrichment [wt%] (The number of fuel rods per FA)** | | **BA content [wt%] (The number of BA rods per FA)** |
|---|---|---|---|
| | **Normal** | **Zoned** | |
| H0 | 4.52 (184) | 4.00 (52) | (0) |
| H1 | 4.50 (176) | 4.00 (52) | 6.0 (8) |
| H2 | 4.50 (172) | 4.00 (52) | 6.0 (12) |
| J0 | 4.48 (184) | 4.00 (52) | (0) |
| J1 | 4.48 (176) | 4.00 (52) | 6.0 (8) |
| J2 | 4.48 (172) | 4.00 (52) | 6.0 (12) |
| K0 | 4.49 (184) | 4.00 (52) | (0) |
| K1 | 4.48 (176) | 4.01 (52) | 6.0 (8) |
| K2 | 4.48 (172) | 4.01 (52) | 6.0 (12) |
| L0 | 4.70 (184) | 4.20 (52) | (0) |
| L1 | 4.70 (176) | 4.20 (52) | 6.0 (8) |
| L2 | 4.70 (172) | 4.20 (52) | 6.0 (12) |
| M0 | 4.70 (184) | 4.20 (52) | (0) |
| M1 | 4.70 (176) | 4.20 (52) | 6.0 (8) |
| M2 | 4.70 (172) | 4.20 (52) | 6.0 (12) |
| N0 | 4.70 (184) | 4.20 (52) | (0) |
| N1 | 4.70 (176) | 4.20 (52) | 6.0 (8) |
| N2 | 4.70 (172) | 4.20 (52) | 6.0 (12) |
| O0 | 4.70 (184) | 4.20 (52) | (0) |
| O1 | 4.70 (176) | 4.20 (52) | 6.0 (8) |
| O2 | 4.70 (172) | 4.20 (52) | 6.0 (12) |
| P0 | 4.70 (184) | 4.20 (52) | (0) |
| P1 | 4.70 (176) | 4.20 (52) | 6.0 (8) |
| P2 | 4.70 (172) | 4.20 (52) | 6.0 (12) |

The numbers of fuel assemblies for each type used in the cycles from 7th to 12th are shown in Table II. These data are the same as in all the cores of the different cases considered in this work. Also, this table shows what types of fuel assemblies are loaded and discharged. At the end of each cycle, sixty-four fuel assemblies are discharged from the core in the order of higher burnup (BU) and the same number of fresh fuel assemblies is loaded at the beginning of the next cycle. The fuel assembly of L0 type is the ATF assembly which is first loaded in the core at the beginning of 8th cycle. The fuel assemblies using ATF rods are indicated by coloring with red. Table III specifies the data of each fuel assembly type for the CASE 1 which uses the conventional $UO_2$ fuel. These data includes the uranium enrichment, burnable absorber (BA) content, and the number of fuel rods and BA rods in each type of fuel assembly. All of fuel assemblies employed an enrichment zoning to reduce the pin power peaking, which places low uranium enrichment fuel rods around the water holes [6]. The BA rods are used to reduce excess reactivity [5]. The pellet of BA rod consists of $UO_2$+$Gd_2O_3$ mixture. The pellet has $UO_2$ of natural uranium enrichment and the $Gd_2O_3$ content is 6.0 wt% in all cases. To make the axial power distribution flatter, the top and bottom of BA rod pellet used cutback material which has only $UO_2$ without $Gd_2O_3$. The configuration of BA rods is indicated in Fig. 1. There are three different types of fuel pin arrangement that are designated by numbers. The numerical type '0' arrangement includes 184 normal fuels and 52 zoned fuels without BA rods. The Types '1' and '2' include normal and zoned fuels with BA rods, which have different number of the fuel rods and BA rods. The pin loading patterns of each type are shown in Fig. 2.

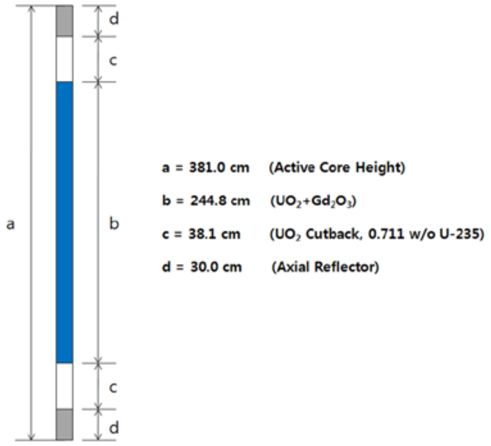

Fig. 1. Axial configuration of burnable absorber rod

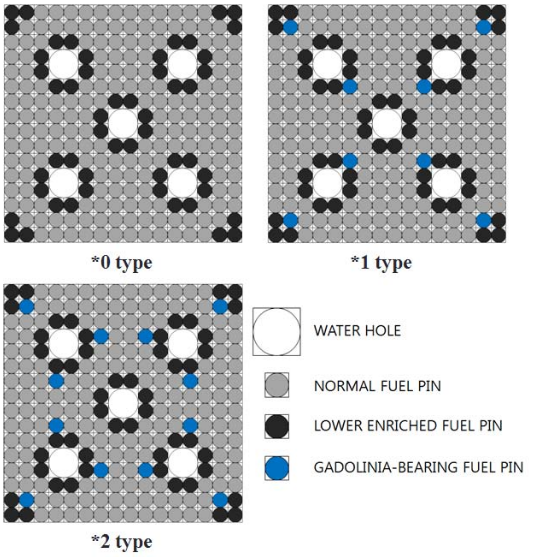

***0 type** ***1 type** ***2 type**

Fig. 2. Pin loading patterns of fuel assemblies for each numerical type

Fig. 3 shows the core loading pattern of 12th cycle (i.e., equilibrium cycle) of the CASE 1. Each color in order of blue, red, and green means fresh, once-burned, and twice-burned fuel assemblies. All cycles from 7th to 12th for all CASEs have same loading pattern as that given in Fig. 3 even if the shuffling schemes are different. The low-leakage loading pattern was considered as partial fuel loading scheme. There are no fresh fuel assemblies in center of the core in order to mitigate the radial power peaking around the center of the core.

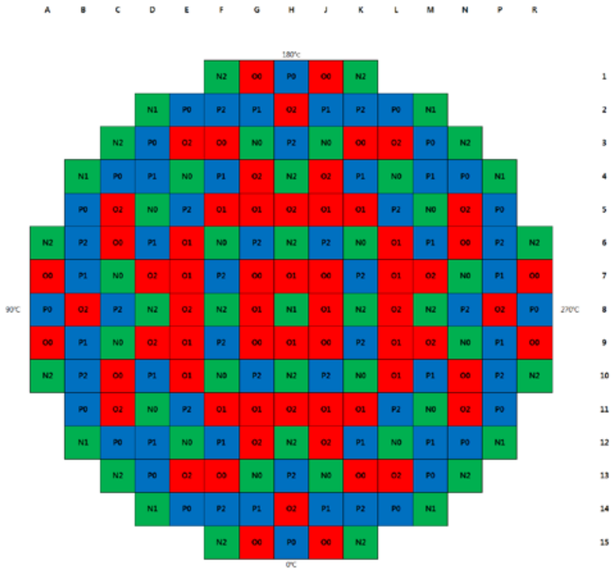

|  | A | B | C | D | E | F | G | H | J | K | L | M | N | P | R |
|---|---|---|---|---|---|---|---|---|---|---|---|---|---|---|---|
| 1 |  |  |  |  |  | N2 | O0 | P0 | O0 | N2 |  |  |  |  |  |
| 2 |  |  |  | N1 | P0 | P2 | P1 | O2 | P1 | P2 | P0 | N1 |  |  |  |
| 3 |  |  | N2 | P0 | O2 | O0 | N0 | P2 | N0 | O0 | O2 | P0 | N2 |  |  |
| 4 |  | N1 | P0 | P1 | N0 | P1 | O2 | N2 | O2 | P1 | N0 | P1 | P0 | N1 |  |
| 5 |  | P0 | O2 | N0 | P2 | O1 | O1 | O2 | O1 | O1 | P2 | N0 | O2 | P0 |  |
| 6 | N2 | P2 | O0 | P1 | O1 | N0 | P2 | N2 | P2 | N0 | O1 | P1 | O0 | P2 | N2 |
| 7 | O0 | P1 | N0 | O2 | O1 | P2 | O0 | O1 | O0 | P2 | O1 | O2 | N0 | P1 | O0 |
| 8 | P0 | O2 | P2 | N2 | O2 | N2 | O1 | N1 | O1 | N2 | O2 | N2 | P2 | O2 | P0 |
| 9 | O0 | P1 | N0 | O2 | O1 | P2 | O0 | O1 | O0 | P2 | O1 | O2 | N0 | P1 | O0 |
| 10 | N2 | P2 | O0 | P1 | O1 | N0 | P2 | N2 | P2 | N0 | O1 | P1 | O0 | P2 | N2 |
| 11 |  | P0 | O2 | N0 | P2 | O1 | O1 | O2 | O1 | O1 | P2 | N0 | O2 | P0 |  |
| 12 |  | N1 | P0 | P1 | N0 | P1 | O2 | N2 | O2 | P1 | N0 | P1 | P0 | N1 |  |
| 13 |  |  | N2 | P0 | O2 | O0 | N0 | P2 | N0 | O0 | O2 | P0 | N2 |  |  |
| 14 |  |  |  | N1 | P0 | P2 | P1 | O2 | P1 | P2 | P0 | N1 |  |  |  |
| 15 |  |  |  |  |  | N2 | O0 | P0 | O0 | N2 |  |  |  |  |  |

Fig. 3. Core loading pattern of beginning of 12th cycle of CASE 1

## 4. Result and Analysis

The reload core analysis from the cycle 7 showed that the equilibrium core is reached from 12th. We analyzed the critical boron concentration (CBC), 3-dimensional peaking factor, axial offset (AO), moderator temperature coefficient (MTC), and shutdown margin (SDM) over time for the 12th cycles of the four cases. Fig. 4 shows the CBC curve for each CASE. The CASE 1 and 4 have similar cycle length about 480 EFPDs because the CASE 4 core is designed to have the similar cycle length at the equilibrium cycle to the reference case (i.e., CASE 1) by increasing uranium enrichment. The CASE 4 has larger CBC than CASE 1 at BOC and rapidly decreased CBC curve because the CASE 4 has higher uranium enrichment and fewer amount of initial heavy metal (HM) which leads to an increase of moderator to fuel (M/F) ratio. The loss of initial HM is resulted from the use of chromium metal in fuel pellet. The CASE 2 and 3 have similar gradient of the CBC curves to the CASE 4 because the amounts of initial HM of three CASEs are almost same. The cycle lengths of the CASE 2 and 3 are estimated to be ~430 EFPDs and 456 EFPDs respectively at equilibrium cycle. The 3-dimensional peaking factors for each CASE are indicated in Fig. 5 below. The maximum peaking factors for all the cases are occurred at BOC. The maximum peaking factor is about 1.9 for CASE 4, which is satisfied within the typical target limit of 2.5. Fig. 6 shows the changes of AO (Axial Offset) over time at the equilibrium cycles. The AO is changed in the range from -0.04 % to 0.08 %.

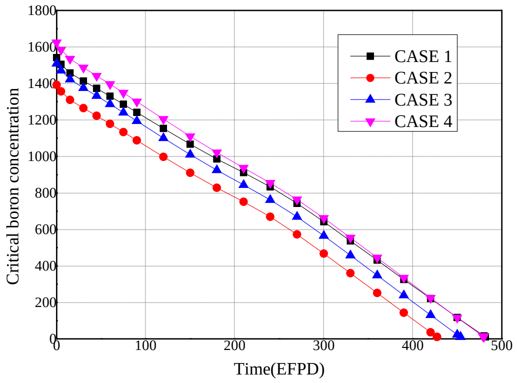

Fig. 4. Comparison of critical boron concentration for each CASE

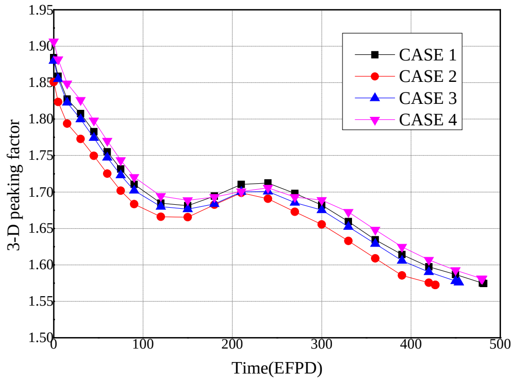

Fig. 5. Comparison of 3-dimensional peaking factor for each CASE

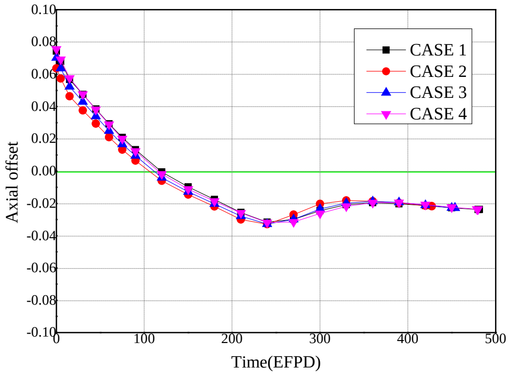

Fig. 6. Comparison of axial offset for each CASE

Table IV shows the MTC for all the cases from 7th to 12th cycles. We considered hot full power (HFP) and hot zero power (HZP) at the same time. While all the MTCs at any time points are negative at HFP, the MTCs on HZP have slightly positive value at BOC. In case of OPR-1000, the positive MTC on HZP has been permitted by +9 pcm/°C[5]. Table V shows the SDM (ShutDown Margin) for all the cases from 7th to 12th cycles. The SDMs for all the cases at any condition are more than 6500 pcm which is the required margin for OPR1000.

Table IV. Comparison of the moderator temperature coefficient for each CASE from 7th to 12th cycles

| Cycle | | CASE 1 | | CASE 2 | | CASE 3 | | CASE 4 | |
|---|---|---|---|---|---|---|---|---|---|
| | | HFP | HZP | HFP | HZP | HFP | HZP | HFP | HZP |
| **7** | **BOC** | -16.07 | 4.90 | -16.07 | 4.90 | -16.07 | 4.90 | -16.07 | 4.90 |
| | **EOC** | -71.01 | -35.47 | -71.01 | -35.47 | -71.01 | -35.47 | -71.01 | -35.47 |
| **8** | **BOC** | -15.09 | 5.33 | -17.14 | 3.93 | -15.78 | 4.82 | -14.61 | 5.55 |
| | **EOC** | -71.13 | -35.45 | -69.32 | -34.19 | -69.95 | -34.69 | -70.49 | -35.19 |
| **9** | **BOC** | -14.59 | 5.64 | -16.39 | 4.33 | -15.01 | 5.18 | -13.75 | 5.91 |
| | **EOC** | -70.28 | -35.18 | -67.44 | -33.25 | -68.37 | -34.04 | -69.29 | -34.77 |
| **10** | **BOC** | -14.12 | 5.91 | -15.38 | 5.08 | -14.06 | 5.78 | -12.92 | 6.43 |
| | **EOC** | -69.70 | -34.92 | -66.45 | -32.63 | -67.59 | -33.60 | -68.57 | -34.51 |
| **11** | **BOC** | -14.02 | 6.01 | -14.57 | 5.64 | -13.49 | 6.24 | -12.41 | 6.78 |
| | **EOC** | -69.71 | -34.93 | -66.35 | -32.63 | -67.49 | -33.63 | -68.50 | -34.53 |
| **12** | **BOC** | -14.09 | 5.96 | -14.80 | 5.45 | -13.65 | 6.08 | -12.57 | 6.63 |
| | **EOC** | -69.67 | -34.92 | -66.36 | -32.63 | -67.53 | -33.59 | -68.53 | -34.54 |

Table V. Comparison of the shutdown margin for each CASE from 7th to 12th cycles

| Cycle | | CASE 1 | | CASE 2 | | CASE 3 | | CASE 4 | |
|---|---|---|---|---|---|---|---|---|---|
| | | HFP | HZP | HFP | HZP | HFP | HZP | HFP | HZP |
| **7** | **BOC** | 7797 | 7961 | 7797 | 7961 | 7797 | 7961 | 7797 | 7961 |
| | **EOC** | 7293 | 8798 | 7293 | 8798 | 7293 | 8798 | 7293 | 8798 |
| **8** | **BOC** | 7739 | 7831 | 7956 | 8154 | 7807 | 7935 | 7664 | 7736 |
| | **EOC** | 7236 | 8765 | 7399 | 8900 | 7291 | 8794 | 7189 | 8694 |
| **9** | **BOC** | 7597 | 7688 | 7804 | 7955 | 7663 | 7774 | 7530 | 7609 |
| | **EOC** | 7151 | 8644 | 7343 | 8755 | 7198 | 8638 | 7062 | 8528 |
| **10** | **BOC** | 7620 | 7707 | 7806 | 7955 | 7673 | 7781 | 7547 | 7621 |
| | **EOC** | 7161 | 8639 | 7318 | 8711 | 7171 | 8596 | 7035 | 8492 |
| **11** | **BOC** | 7619 | 7702 | 7838 | 7978 | 7694 | 7793 | 7557 | 7621 |
| | **EOC** | 7158 | 8634 | 7316 | 8703 | 7167 | 8588 | 7029 | 8481 |
| **12** | **BOC** | 7619 | 7701 | 7834 | 7971 | 7689 | 7786 | 7552 | 7615 |
| | **EOC** | 7159 | 8635 | 7321 | 8708 | 7171 | 8591 | 7030 | 8483 |

Table VI show the average burnup for each FA type and for all of FAs at EOC of 12th cycle. The BU is determined by the amount of initial HM and uranium enrichment. CASE 1 has lower BU in all rows than CASE 4 which has same cycle length about 480 EFPDs. In CASE 4, the higher BU is required to satisfy the cycle length because it has fewer amount of initial HM than CASE 1. The BU is increased in order of CASE 2, 3, and 4 which have same amount of initial HM and increasing uranium enrichment.

Table VI. Average burnup for each FA type and for all FAs at the end of 12th cycle

| FA type | Average BU [MWD/kgU] | | | |
|---|---|---|---|---|
| | CASE 1 | CASE 2 | CASE 3 | CASE 4 |
| **N0** | 53.39 | 49.07 | 52.20 | 55.27 |
| **N1** | 49.52 | 45.66 | 48.45 | 51.20 |
| **N2** | 51.35 | 47.36 | 50.23 | 53.05 |
| **O0** | 35.36 | 32.22 | 34.45 | 36.64 |
| **O1** | 42.94 | 39.66 | 42.07 | 44.43 |
| **O2** | 41.20 | 37.92 | 40.30 | 42.63 |
| **P1** | 17.69 | 15.88 | 17.10 | 18.31 |
| **P2** | 23.70 | 21.52 | 23.03 | 24.52 |
| **P3** | 22.36 | 20.36 | 21.74 | 23.10 |
| **Total** | 36.50 | 33.47 | 35.63 | 37.76 |

## 5. Conclusion

In this work, we studied the PWR cores which are loaded with ATF assemblies to improve the safety of reactor core. The ATF rod consists of the metallic microcell $UO_2$ pellet which includes chromium of 3.34 wt% and the outer 0.05mm thick coating of Cr-based alloy with atomic number ratio of 85:15. We performed the cycle-by-cycle reload core analysis from the cycle 8 at which the ATF fuel assemblies start to be loaded into the core. The target nuclear power plant is the Hanbit-3 nuclear power plant. From the analysis, it was found that 1) the uranium enrichment is required to be increased up to 5.20/4.70 wt% in order to satisfy a required cycle length of 480 EFPDs, 2) the cycle length for the core using ATF fuel assemblies with the same uranium enrichments as those in the reference $UO_2$ fueled core is decreased from 480 EFPDs to 430 EFPDs, 3) the cycle length of the ATF fueled core with an limiting uranium enrichments of 4.95/4.45wt% is about 456 EFPDs, and 4) there were no degradations of the ATF fueled cores except for the reduction of the cycle length. In the future, the effect of ATF pellet density and size will be investigated.

## Acknowledgement

This work was supported by the National Research Foundation of Korea (NRF) funded by the Korea government (MSIP) (NRF-2012M2A8A5025824).

## REFERENCES

[1] Dong-Joo Kim, Young Woo Rhee, Jong Hun Kim, Keon Sik Kim, Jang Soo Oh, Jae Ho Yang, Yang-Hyun Koo, Kun-Woo Song, “Fabrication of micro-cell $UO_2$-Mo pellet with enhanced thermal conductivity,” Journal of Nuclear Materials 462 (2015) 289-295.

[2] Hyun-Gil Kim, Il-Hyun Kim, Yang-Il Jung, Dong-Jun Park, Jeong-Yong Park, Yang-Hyun Koo, “Adhesion property and high-temperature oxidation behavior of Cr-coated

Zircaloy-4 cladding tube prepared by 3D laser coating," Journal of Nuclear Materials 465 (2015) 531-539.
[3] J. Y. Cho et al., "DeCART2D v1.0 User's Manual," KAERI/TR-5116/2013.
[4] J. Y. Cho et al., "MASTER 3.0 USER'S MANUAL," KAERI/UM-8/2004.
[5] T.H. Jeon et al., "Core Design and Safety Analysis of Dual-Cooled Annular Fuel for OPR-1000," KAERI/TR-3762/2009.
[6] DaeHee HWANG and Ser Gi Hong, "An Optimization Study of LWR Fuel Assembly Design for TRU Burning using FCM and UO2-ThO2 Fuel Pins," Transactions of the Korean Nuclear Society Spring Meeting Jeju, Korea, May 29-30, 2014.